Photoinduced Electron-Transfer Processes of Tetrathiafulvalene-(Spacer)-(Naphthalenediimide)-(Spacer)-Tertrathiafulvalene Triads in Solution

Xuefeng Guo,[†] Zhenhai Gan,[‡] Hongxia Luo,[‡] Yasuyuki Araki,[‡] Deqing Zhang,*[,†] Daoben Zhu,*[,†] and Osamu Ito*[,‡]

Center for Molecular Sciences, Institute of Chemistry, Chinese Accademy Science, Bejing, 100080 China, and Institute of Multidisciplinary Research for Advanced Materials, Tohoku University, CREST (JST), Katahira, Aoba-ku, Sendai, 980-8577 Japan

Received: August 2, 2003; In Final Form: September 18, 2003

Intramolecular photoinduced charge-separation and charge-recombination processes of tetrathiafulvalene-(spacer)-naphthalenediimide-(spacer)-tertrathiafulvalenetriads (TTF-(sp)-NIm-(sp)-TTF), which have been designed to change the length and kind of the spacers, have been investigated in various solvents by time-resolved absorption and fluorescence techniques. The fluorescence lifetimes of the NIm moiety considerably decreased compared with that of the NIm molecule, suggesting the photoinduced intramolecular charge-separation via the singlet excited state of the NIm moiety. From the observed short fluorescence lifetimes, the charge-separation rate constants (k_{CS}) and quantum yields (Φ_{CS}) of TTF-(sp)-NIm-(sp)-TTF have been evaluated; the k_{CS} values for the triads with the rigid cyclohexyl spacers are larger than that with long flexible alkyl chain spacers. In the nanosecond transient spectra in PhCN, the absorption bands were observed at 480 and 760 nm, which were attributed to the radical anion of NIm ($NIm^{\bullet-}$) suggesting the formation of $TTF^{\bullet+}$-(sp)-$NIm^{\bullet-}$-(sp)-TTF. From the decays of the radical ion-pair, the charge-recombination rate-constants (k_{CR}) were evaluated in the range of $9 \times 10^5 - 3 \times 10^7$ s^{-1}. Longer lifetimes of the radical ion-pair were observed for the triads with the cyclohexyl spacer than that of the long flexible spacer. From the temperature dependence of the k_{CR} values, the reorganization energies and coupling constants were experimentally evaluated in PhCN; small coupling constants of the triads with the cyclohexyl spacers than that of the long flexible spacers support the relatively long lifetimes of the charge separated states of the chyclohexyl spacer.

Introduction

Since the discovery of donor and acceptor systems which are very attractive with unique photophysical and electrochemical properties, considerable efforts have been devoted in recent years to the development of covalently linked donor−acceptor systems.[1] Such molecular systems are of particular interest in that they can exhibit characteristic electronic and excited-state properties, which make them promising candidates for the investigations of photoinduced electron-transfer processes and long-lived charge-separated states.[2,3] These phenomena open potential applications in the realization of new molecular electronic devices[4] and photovoltaic cells.[5] In these intramolecular processes involving electron transfer between both electroactive entities, the diimide derivatives (Im) appear to be of special interese as an efficient electron acceptor in such devices because of its good ability as an electron acceptor and the characteristic sharp absorption bands of the radical anions, which do not overlap with other transient species.[6] Thus, in the present study, we employed naphthalenediimide (NIm) derivatives as an electron acceptor.

Among the wide variety of donor molecules, the tetrathiafulvalene (TTF) derivatives are interesting classes of compounds in the light of the photoinduced intermolecular electron transfer in the presence of electron acceptors such as fullerenes.[7,8] In the TTF-(spacer)-acceptor dyads, intramolecular charge-separated states ($TTF^{\bullet+}$-(spacer)-$acceptor^{\bullet-}$) have also been revealed, when the C_{60} derivatives were employed as acceptors.[8] This peculiarity of the good electron donor ability of the TTF derivatives is thought to be because of the gain of aromaticity as a result of the formation of the very stable heteroaromatic 1,3-dithiolium cation(s) upon oxidation(s) of the TTF molecule which is nonaromatic in its neutral form.[8] On this basis, the TTF derivatives have been covalently linked to the NIm moiety through the spacers with saturated bonds, expecting efficient photoinduced charge-separation with long lifetime radical ion-pairs.

Following a strategy which consists of controlling the distance between both counterparts, TTF-(sp)-NIm-(sp)-TTF triads were prepared as shown in Chart 1, in which two kinds of spacers (sp) were chosen; one was long flexible dodecyl group and another was rigid cyclohexyl group (Supporting Information). To improve the solubility and fabrications, the other side of the TTF moieties are connected with long alkyl chains as shown in Chart 1. Thereby, through-bond interactions which are of great importance for photoinduced electron-transfer processes are expected to be controlled by flexible and rigid spacers. Thus, in the present study, we investigated the photoinduced charge-separation and charge-recombination processes in the TTF-(sp)-NIm-(sp)-TTF triads by the measurements of fluorescence lifetimes and transient absorption spectroscopy. The temperature

* To whom correspondence should be addressed. E-mail: dqzhang@iccas.ac.cn; ito@tagen.tohoku.ac.jp.
[†] Chinese Accademy Sciences.
[‡] Tohoku University.

10.1021/jp0362638 CCC: $25.00
Published on Web 10/24/2003

CHART 1

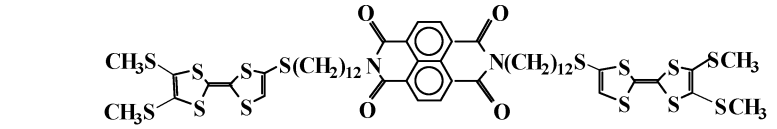

1

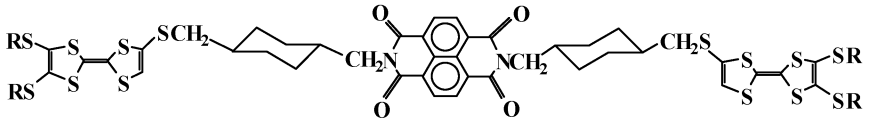

2 $R = CH_3$; **3** $R = -CH_2CH(CH_2CH_3)_2$

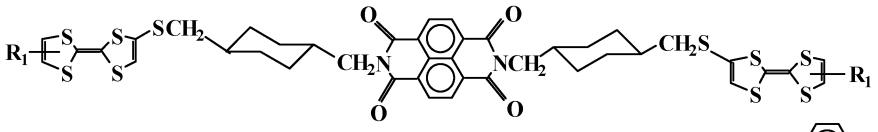

4

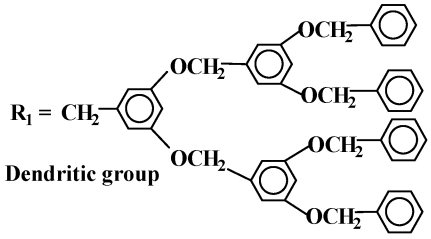

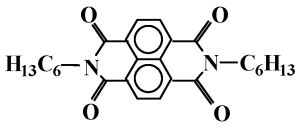

5

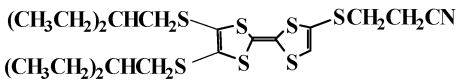

6

dependence of the rate constants gave precise parameters to discuss the electron-transfer processes on the basis of Marcus theory.[9]

Experimental Section

Materials. TTF-(sp)-NIm-(sp)-TTF triads (**1**−**4**) were synthesized by methods summarized in the Supporting Information. The NIm derivative (**5**) and TTF derivative (**6**) were also prepared according to the methods described in the Supporting Information. Tetrakis(diethylamino)ethylene (TDAE) and solvents are all the best grade commercially available.

Molecular Orbital Calculations. The optimized structure of the neutral molecule was calculated with the PM-3 level in MOPAC.[10] The energy levels and the electron densities of the HOMO and LUMO were calculated by Gaussian 98 (HF/3-21G level).

Measurements. *Steady-State Measurements.* Steady-state absorption spectra in the visible and near-IR regions were measured on a JASCO V530 spectrophotometer in a 1 cm quartz cell. Steady-state fluorescence spectra of the samples were measured on a Shimadzu RF-5300PC spectrofluorophotometer.

Time-Resolved Fluorescence Measurements. The lifetimes of the fluorescence bands were measured by a single-photon counting method using a second harmonic generation (SHG, 410 nm) of a Ti:sapphire laser (Spectra-Physics, Tsunami 3950-L2S, 1.5 ps fwhm) and a streakscope (Hamamatsu Photonics, C43334−01) equipped with a polychromator (Action Research, SpectraPro 150) as an excitation source and a detector, respectively.[11] Lifetimes were evaluated with software attached to the equipment.

Nanosecond Transient Absorption Measurements. Nanosecond transient absorption measurements were carried out using the SHG (532 nm) of a Nd:YAG laser (Spectra-Physics, Quanta-Ray GCR-130, 6 ns fwhm) as an excitation source. For transient absorption spectra in the near-IR region (600∼1000 nm) and the time-profiles, monitoring light from a pulsed Xe-lamp was detected with a Ge-APD (Hamamatsu Photonics, B2834).[11] For spectra in the visible region (400∼600 nm), a Si−PIN photodiode (Hamamatsu Photonics, S1722-02) was used as a detector.[11]

All of the samples in a quartz cell (1× 1 cm) were deaerated by bubbling Ar gas through the solution for 10 min.

Results and Discussion

Molecular Orbital Calculations. Optimized structures of **1**−**3** are shown in Figure 1. For **1** with flexible single chains, the extended structure has minimum energy. For **2**−**4**, according to the starting configurations with respect to cyclohexyl ring (axial and equatorial), different structures have minimum energies. Among them, the typical configurations for **2** and **3** with minimum energies are shown in Figure 1; **2** and **3** have almost similar structures.[12] Two TTF planes have different orientations with respect to the NIm moiety. The structural difference between **2** and **3** due to the length of alkyl chains at the terminals of the TTF moieties of the opposite position to the cyclohexyl spacers seems to be small. For **4** with dendron groups at the terminals of the TTF moieties, a similar mixture structure to **3** was evaluated.

The electron densities of the HOMO and LUMO of **1**−**3** are shown in Figure 1, in which the HOMO localizes on one of the

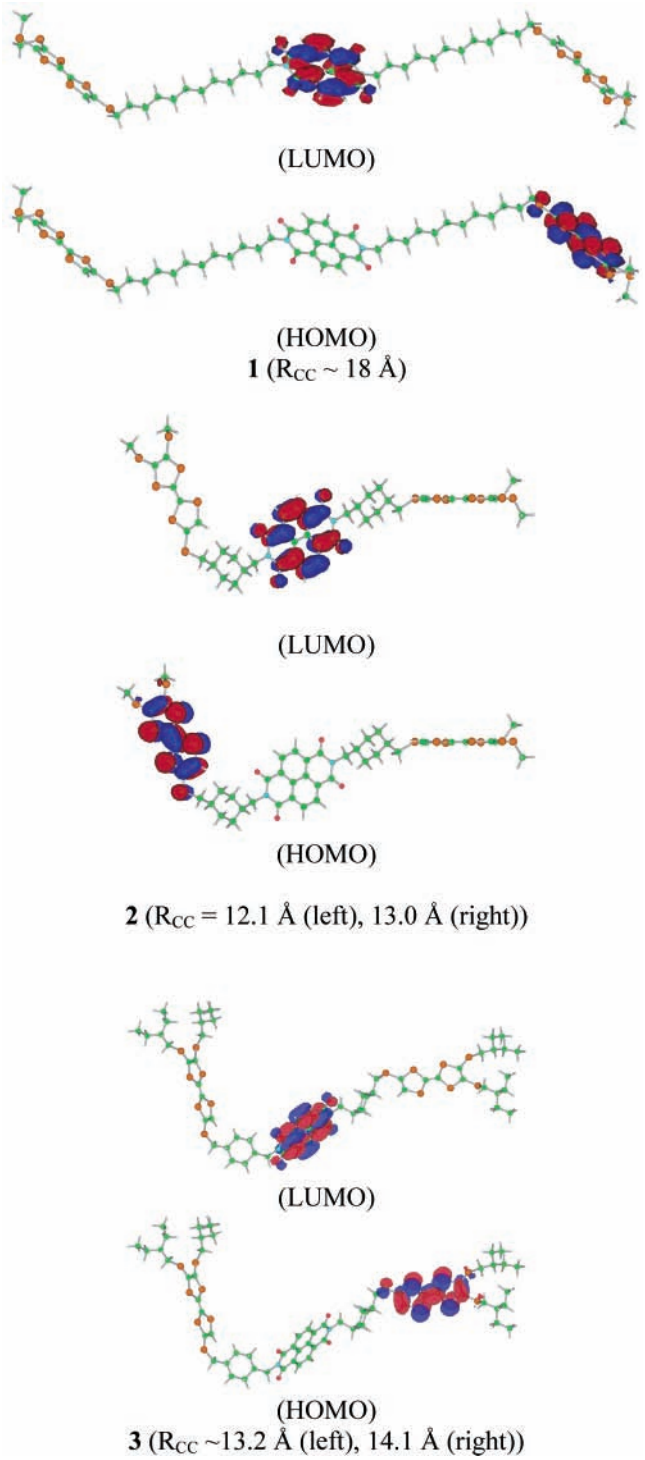

Figure 1. Optimized molecular structures, the MOMO and LUMO electron densities, and center-to-center distance (R_{cc}).

TTF moieties, which corresponds to the distribution of the hole (radical cation) in the charge-separated state. On the other hand, the LUMO localizes on the central NIm moiety, which corresponds to the distribution of the electron (radical anion) in the charge-separated state.

From the optimized structures, the distance between the center of the NIm moiety and the center of one of the TTF moieties (R_{cc}) was evaluated as listed in Table 1, in which the oxidation and reduction potentials are also listed.

Absorption and Fluorescence Spectra. Steady-state absorption spectra of triad **3**, a model of the NIm moiety **5**, and a model of the TTF moiety **6** in PhCN are shown in Figure 2.

TABLE 1: Reduction Potentials (E_{red}) and Oxidation Potentials (E_{ox}) of Triad 1−4, R_{CC}

compound	E_{red}/V[a]	E_{ox}/V[a]	R_{CC}/Å[b]
1	−0.83	0.46	18
2	−0.84	0.48	12.1 (13.0)
3	−0.85	0.47	13.2 (14.1)
4	−0.85	0.46	13.2 (14.1)

[a] Potentials vs SCE, in $CHCl_3$ and E_{red} of **5** (−0.85 eV) and E_{ox} of **6** (0.46 eV). [b] Shorter R_{CC} values in Figure 1 were employed for the calculation of the free-energy changes in Tables 2 and 3.

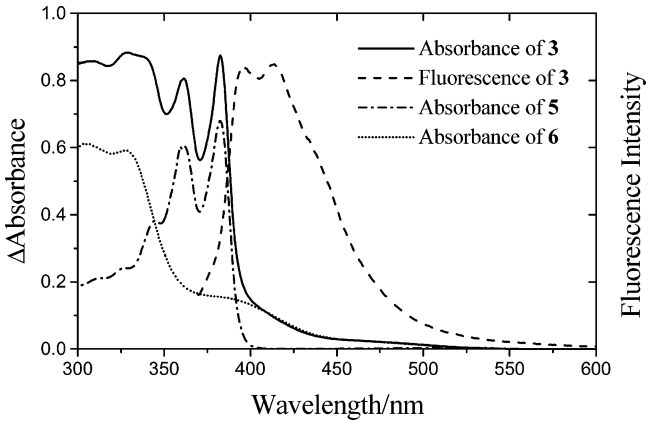

Figure 2. Absorption spectra and fluorescence spectra of **3** (0.02 mM), **5**(0.02 mM), and **6** (0.02 mM) in toluene.

The NIm moiety of **5** shows the absorption band at 360 and 380 nm. The TTF moiety of **6** shows the absorption band at 340 nm with a shoulder at 400 nm. The absorption bands of triad **3** observed in these wavelength region are almost overlapping the NIm moiety with the TTF moiety, suggesting no appreciable interaction between the TTF and NIm moieties in the ground states, because of the long distance between the both moieties. The nanosecond laser light (355 nm) from the THG of YAG laser predominantly excites the NIm moiety in the triads.

Fluorescence spectra of **1**−**5** were observed in the visible region by steady-state measurements; an example of the observed fluorescence spectrum is shown in Figure 2 for **3** in toluene. The shape of the fluorescence spectrum of **3** is almost the same as that of **5**, although the fluorescence intensity of **3** is weaker than that of **5**. Each fluorescence spectrum is a mirror image of the absorption of the NIm moiety. Thus, these fluorescence bands in the region of 400−500 nm arise from the excited singlet state of the NIm moiety.

Fluorescence Lifetimes. In Figure 3, the time profiles of the fluorescence intensity at the peak position of triads **1**, **3**, and **5** in PhCN are shown. Although the isolated NIm molecule (**5**) showed the initial quick fluorescence decay, its partition relative to the slow fluorescence decay part is small in PhCN. In the case of **1** with flexible long spacers, a typical two-component exponential decay was observed in PhCN, although a single-exponential decay was observed in toluene. For triad **3** with the cyclohexyl spacers, fluorescence decays showed a single exponential. These data are summarized in Table 2.

From the lifetimes, the charge-separation rate constants (k_{CS}) and quantum yields (Φ_{CS}) have been evaluated from the following relations:

$$k_{CS} = (1/\tau_f)_{sample} - (1/\tau_f)_{ref} \quad (1)$$

$$\Phi_{CS} = [(1/\tau_f)_{sample} - (1/\tau_f)_{ref}]/(1/\tau)_{sample} \quad (2)$$

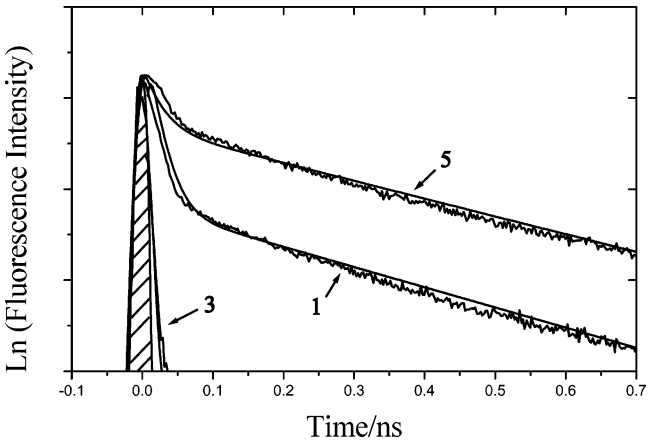

Figure 3. Fluorescence time profiles of **1**, **3**, and **5** in PhCN.

TABLE 2: Fluorescence Lifetime (τ_f), Charge-Separation Rate-Constants (k_{CS}),[a] Charge-Separation Quantum-Yields (Φ_{CS}),[b] and Free-Energy Changes for Charge-Separation ($-\Delta G_{CS}$)[c] of TTF-(sp)-NIm-(sp)-TTF in Toluene, $CHCl_3$, and PhCN

compound	solvent	τ_f/ps	k_{CS}/M^{-1} s^{-1}	Φ_{CS}	$-\Delta G_{CS}$/eV
1	toluene	520 (100%)	1.6×10^9	0.82	1.12
	$CHCl_3$	97 (84%) 1700 (16%)	9.9×10^9	0.96	1.46
	PhCN	95 (83%) 2180 (17%)	9.7×10^9	0.92	1.73
2	toluene	320 (100%)	2.7×10^9	0.89	1.32
	$CHCl_3$	84 (100%)	11.4×10^9	0.96	1.57
	PhCN	41 (100%)	23.5×10^9	0.97	1.77
3	toluene	200 (100%)	4.6×10^9	0.93	1.28
	CHC_3	53 (100%)	18.4×10^9	0.98	1.55
	PhCN	34 (100%)	28.5×10^9	0.97	1.77
4	toluene	180 (100%)	5.2×10^9	0.94	1.27
	$CHCl_3$	44 (100%)	22.3×10^9	0.98	1.54
	PhCN	38 (100%)	25.5×10^9	0.97	1.76

[a] $k_{CS} = (1/\tau_f)_{sample} - (1/\tau_f)_{ref}$; $(\tau_f)_{ref}$ = 2860 ps (toluene), 2200 ps ($CHCl_3$), and 1160 ps (PhCN). [b] $\Phi_{CS} = [(1/\tau_f)_{sample} - (1/\tau_f)_{ref}]/(1/\tau)_{sample}$. [c] $-\Delta G_{CS} = \Delta E_{0-0} - E_{ox} + E_{red} - \Delta G_S$; $\Delta G_S = e^2/(4\pi\Delta\epsilon_0)[(1/2R_+ + 1/2R_- - 1/R_{cc})1/\epsilon_s - (1/2R_+ + 1/2R_-)1/\epsilon_r]$, where ΔE_{0-0} is energy of the 0−0 transition of (3.10 eV), E_{ox} and E_{red} are the first oxidation potential of the donor and the first reduction potential of the acceptor in *o*-dichlorobenzene, respectively, R_+ and R_- are radii of the ion radicals of TTF (7.6 Å) and NIm (5.1 Å), respectively, R_{cc} is the center-to-center distance between the two moieties evaluated from MO calculation (Figure 1), and ϵ_s and ϵ_r are static dielectric constants of solvents used for the rate measurements and the redox potential measurements, respectively.

For compounds with two τ_f values, the average lifetimes calculated by multiplying the fractions were employed for the calculations of k_{CS} and Φ_{CS} values using eqs 1 and 2. The k_{CS} and Φ_{CS} values were evaluated as listed in Table 2, in which the k_{CS} values of TTF-(sp)-NIm-(sp)-TTF triads in toluene were in the region of $(1.6-5.2) \times 10^9$ s^{-1}, whereas in chloroform and PhCN, the k_{CS} values increased almost one order. Triad **1** with the flexible long bond has smaller k_{CS} values even in polar solvents compared with other triads (**2**−**4**) with the cyclohexyl spacers. The Φ_{CS} values of TTF-(sp)-NIm-(sp)-TTF triads are quite high, suggesting that the charge-separation process takes place predominantly via the singlet excited state of the central NIm moiety (^{1}NIm*). For triads (**2**−**4**) with the cyclohexyl spacers, appreciable changes were not observed for the k_{CS} and Φ_{CS} values in all solvents.

Compared with the free-energy of charge-separation ($-\Delta G_{CS}$) in Table 2, the k_{CS} values for (**2**−**4**) increase with $-\Delta G_{CS}$ values, suggesting that the charge-separation process via the ^{1}NIm* moiety may be in the normal region of the Marcus Parabola,[9]

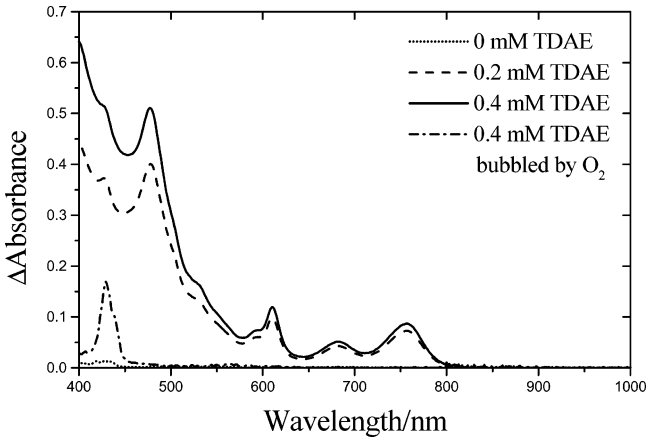

Figure 4. Absorption spectra of **5** (0.02 mM) with different concentrations of tetrakis(dimethylamino)ethylene (TDAE) in PhCN.

suggesting that the reorganization energy (λ_{CS}) value may be larger than ca. 1.8 eV. For **1**, the k_{CS} values seem to saturate near $-\Delta G_{CS}$ values of 1.5−1.7 eV, suggesting a slightly small λ_{CS} for **1**. Larger k_{CS} values for (**2**−**4**) than those for **1** may be attributed to the large coupling constant ($|V|_{CS}$) for the charge-separation process via the ^{1}NIm* moiety; on the other hand, the small k_{CS} value for **1** with the longer spacer may be due to smaller $|V|_{CS}$ than those of **2**−**4** with a shorter rigid spacer.[9]

Absorption Spectra of NIm$^{\bullet-}$. To assign the absorption bands of the radical ion-pairs generated by the laser flash photolysis, the steady-state absorption spectra of the radical anion of **5** (NIm$^{\bullet-}$) were observed by the chemical reduction of **5** with strong electron donors such as tetrakis(diethylamino)-ethylene (TDAE) in polar solvent.[13] As shown in Figure 4, new absorption peaks appeared at 760, 680, 610, and 480 nm. They are all attributed to NIm$^{\bullet-}$, because the cation radical of TDAE does not have an appreciable absorption band in the visible region. The extra peak at 430 nm is due to TDAE. On addition of O_2 into Ar-saturated solution, all of the absorption bands in the 480−760 nm region disappeared quickly, indicating that NIm$^{\bullet-}$ is very sensitive to O_2 probably because of electron transfer from NIm$^{\bullet-}$ to O_2, producing $O_2^{\bullet-}$.

Nanosecond Transient Absorption Measurements. Transient absorption spectra observed by the nanosecond laser excitation (355 nm) of triad **1** in PhCN are shown in Figure 5. Immediately after the laser pulse exposure, the transient absorption bands were observed at 480 and 760 nm at 10 ns. The main two absorption bands at 480 and 760 nm were attributed to the NIm$^{\bullet-}$ moiety. As two weak bands at 600 and 680 nm were also in good agreement with those in Figure 4, they are also attributable to NIm$^{\bullet-}$. Because of absorption bands of the radical cation of the TTF moiety (TTF$^{\bullet+}$), weak bands in the 450−550 nm with a shoulder at 610 nm were reported.[14] These bands of the TTF$^{\bullet+}$ moiety may be overlapped with the absorption bands of the NIm$^{\bullet-}$ moiety. These findings indicate the formation of the charge-separated state (TTF$^{\bullet+}$-(sp)-NIm$^{\bullet-}$-(sp)-TTF). The transient spectra of the radical ions disappeared quickly at 250 ns, indicating a relatively short lifetime of the charge-separated state of **1** even in polar PhCN.

The time profiles at 480 and 760 nm are shown in Figure 5. Because the rises of the 480 and 760 nm bands are quite quick just after the 355 nm laser light pulse, TTF$^{\bullet+}$-(sp)-NIm$^{\bullet-}$-(sp)-TTF of **1** may be produced via the singlet excited state of the NIm moiety. If TTF$^{\bullet+}$-(sp)-NIm$^{\bullet-}$-(sp)-TTF of **1** was produced via the triplet state of the NIm moiety, the slow rises of the absorption bands of the radical ions may be observed. The shoulder in the longer wavelength than the 760 nm band, which

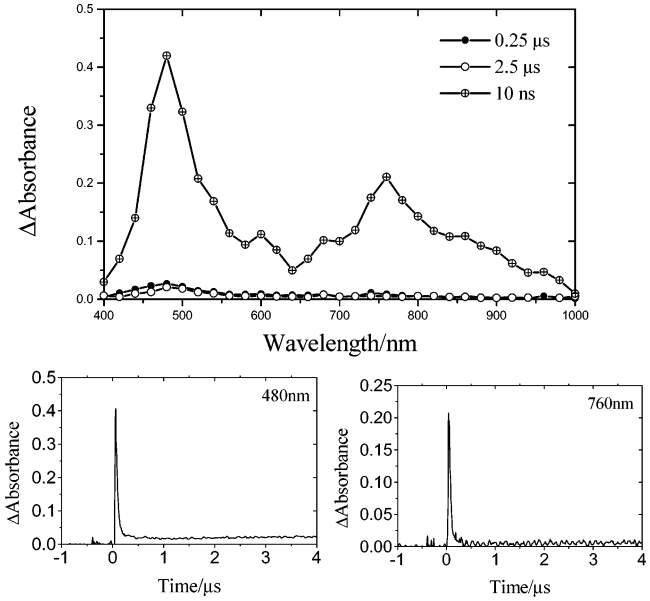

Figure 5. (Upper panel) Transient absorption spectra observed by the 355 nm laser excitation of **1** (0.1 mM) in deaerated PhCN. (Lower panel) Time profiles at 480 and 740 nm of **1**.

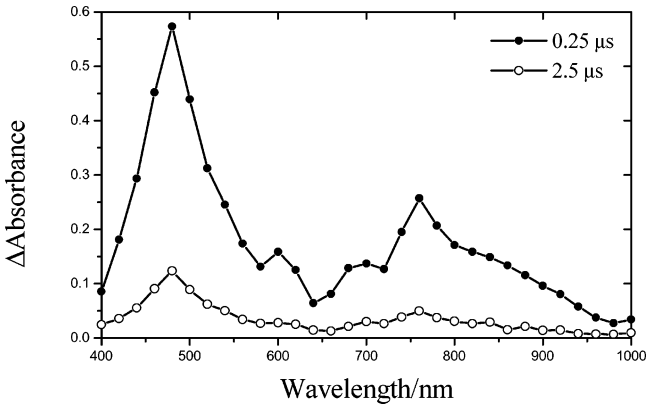

Figure 6. Transient absorption spectraobserved by the 355 nm laser excitation of **3** (0.1 mM) in deaerated PhCN.

was not observed for $NIm^{\bullet-}$ in Figure 4, was characteristic of the transient spectra of $TTF^{\bullet+}$-(sp)-$NIm^{\bullet-}$-(sp)-TTF (**1**). Although the band between 800 and 1000 nm was not reported for the $TTF^{\bullet+}$ moiety in the literature,[14] weak absorption bands were sometimes observed for the $TTF^{\bullet+}$ derivatives in the near-IR region in our previous papers.[7]

From the decays of the 480 and 760 nm bands, the rate constant for charge recombination (k_{CR}) for $TTF^{\bullet+}$-(sp)-$NIm^{\bullet-}$-(sp)-TTF of **1** was evaluated to be 2.9×10^7 s^{-1} in PhCN at room temperature, which corresponds to the lifetime of the radical ion-pair (τ_{RIP}) of 34 ns. In chloroform, similar transient spectra and decay time profiles were observed, giving $\tau_{RIP} =$ 49 ns, which is slightly longer than that in PhCN. In toluene, on the other hand, no transient spectra was observed, suggesting τ_{RIP} is shorter than 6 ns which is the laser pulse width.

The transient spectra observed by the laser excitation of triad **3** with the cyclohexyl spacers in TTF-(sp)-NIm-(sp)-TTF are shown in Figure 6. Because the transient absorption spectrum observed at 250 ns was almost the same as the spectrum at 10 ns for **1** in Figure 5, the formation of $TTF^{\bullet+}$-(sp)-$NIm^{\bullet-}$-(sp)-TTF was also confirmed for **3**. Similar transient absorption bands were observed for **2** and **4** in PhCN. Even in less polar solvents such as chloroform, similar transient absorption spectra were observed for **2**−**4**. However, in nonpolar solvents such as toluene, the transient absorption spectrum was not observed even for **2**−**4** within the time resolution of the laser light pulse (6 ns).

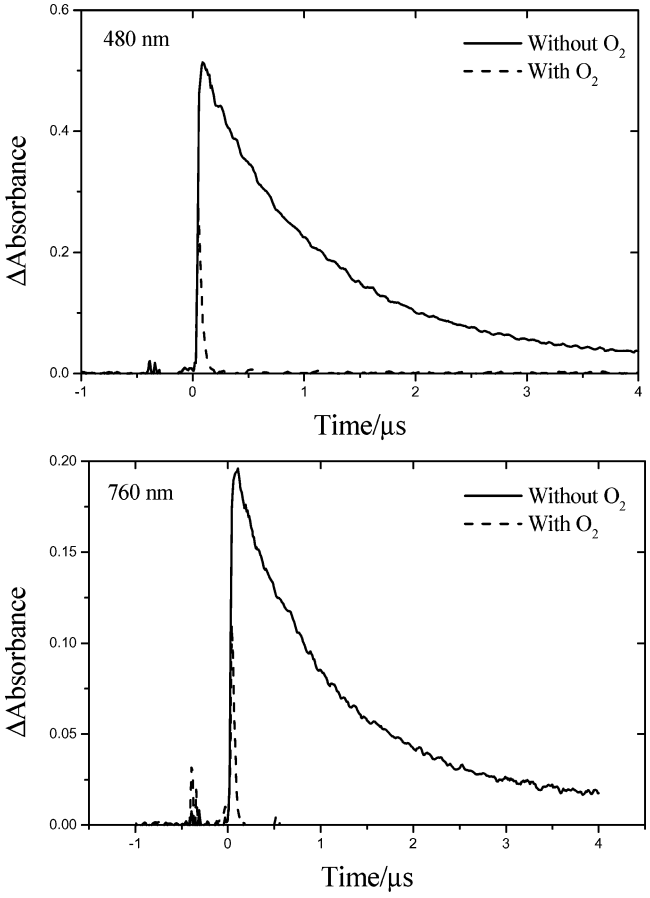

Figure 7. Time profiles at 480 and 760 nm of **3** (0.1 mM) in Ar- and O_2-saturated PhCN.

TABLE 3: Charge-Recombination Rate-Constants (k_{CR}), Lifetimes of Ion-Pair ($\tau_{ion-pair}$), and Free-Energy Changes for Charge-Separation (ΔG_{CR}) of TTF-(sp)-NIm-(sp)-TTF in $CHCl_3$ and PhCN

compound	solvent	k_{CR}/s^{-1}	$\tau_{ion-pair}$/ns	$-\Delta G_{CR}$/eV
1	$CHCl_3$	2.03×10^7	49	1.64
	PhCN	2.90×10^7	34	1.37
2	$CHCl_3$	3.00×10^6	330	1.57
	PhCN	1.78×10^6	560	1.33
3	$CHCl_3$	3.15×10^6	320	1.55
	PhCN	9.07×10^5	1100	1.33
4	$CHCl_3$	5.26×10^6	190	1.56
	PhCN	1.74×10^6	580	1.34

Time profiles of the bands at 480 and 760 nm of the $NIm^{\bullet-}$ moiety for **3** are shown in Figure 7. The decays of the 480 and 760 nm bands were very slow, suggesting the long lifetime of $TTF^{\bullet+}$-(sp)-$NIm^{\bullet-}$-(sp)-TTF for **3**. On addition of O_2, the decay rates of these bands were increased very much, suggesting that the $NIm^{\bullet-}$ moiety is quite sensitive to O_2, which is in good agreement with the O_2 effect on the steady-state measurement as shown in Figure 4. In the case of the $NIm^{\bullet-}$ moiety in **1**, a slight O_2 acceleration effect for the decay curves was also observed; the difference was small, because the original decay of $TTF^{\bullet+}$-(sp)-$NIm^{\bullet-}$-(sp)-TTF for **1** was as fast as O_2 acceleration. The k_{CR} and τ_{RIP} values in the absence of O_2 are summarized in Table 3 with the free-energy changes of charge-recombination ($-\Delta G_{CR}$). The k_{CR} values of **2**−**4** were evaluated to be $(0.91-1.78) \times 10^6$ s^{-1} in PhCN at room temperature, which are more than one order smaller than that of **1**. This

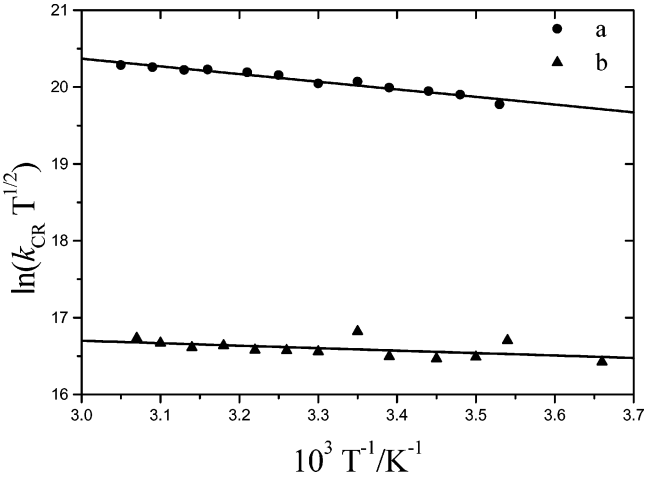

Figure 8. Plots of the semiempirical Marcus equation; (a) **1** and (b) **3** in deaerated PhCN.

TABLE 4: Activation Free-Energies ($\Delta G^{\ddagger}_{CR}$), Reorganization Energies (λ_{CR}), and Coupling Constants ($|V|_{CR}$) for the Charge-Recombination Process for TTF-(sp)-NIm-(sp)-TTF in PhCN

compound	$\Delta G^{\ddagger}_{CR}$/eV	λ_{CR}/eV	$\lvert V\rvert_{CR}$/cm^{-1}
1	0.086	0.80	0.38
2	0.061	0.92	0.10
3	0.025	1.06	0.07
4	0.069	1.01	0.12

indicates that the flexible long spaces accelerate the charge-recombination rates. To reveal the reasons, we tried to evaluate experimentally the (λ) and $|V|$ values for charge-recombination from the temperature changes of the k_{CR} values.

Temperature Effects. More detail parameters for electron transfer can be evaluated by the temperature changes of the rate constants. In general, the free-energy barrier ($\Delta G^{\ddagger}$) for the electron-transfer process can be estimated by measuring the temperature dependence of the electron-transfer rate constant (k). From a semiclassical Marcus eq 3,[9] the k value can be described as follows:

$$\ln(k\sqrt{T}) = \ln\left(\frac{2\pi^{3/2}|V|^2}{h\sqrt{\lambda k_B}}\right) - \frac{\Delta G^{\ddagger}}{k_B T} \qquad (3)$$

where T, h, and k_B are the absolute temperature, Planck's constant, and Boltzman's constant, respectively. The plots of eq 3 for the k_{CR} values of **1** and **3** in PhCN are shown in Figure 8, which exhibits linear relations between $\ln(k_{CR}T^{1/2})$ vs $1/T$. Only in PhCN, reliable temperature changes of the k_{CR} values were observed with low noise. Because PhCN solidified to white polycrystals at a temperature lower than -10 °C, the temperatures were changed to the 0−30 °C region, in which the k_{CR} values were varied from 1.73×10^7 to 4.62×10^7 s^{-1} for **1** and from 0.87×10^6 to 1.10×10^6 s^{-1} for **3**. These changes in the k_{CR} values are larger than the experimental error of our equipment. From the slopes ($-\Delta G^{\ddagger}_{CR}/k_B$), the $\Delta G^{\ddagger}_{CR}$ values were estimated to be 0.10−0.02 eV for **1**−**4** in PhCN (Table 4); the largest $\Delta G^{\ddagger}_{CR}$ value was evaluated for **1**, and the smallest $\Delta G^{\ddagger}_{CR}$ value was for **3**. The λ value was calculated from the following relation:[9]

$$\Delta G^{\ddagger} = \frac{(\Delta G_{CR} + \lambda)^2}{4\lambda} \qquad (4)$$

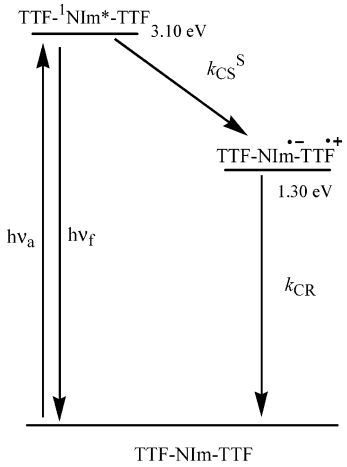

Figure 9. Energy diagram of triads in PhCN; TTF-NIm-TTF = TTF-(sp)-NIm-(sp)-TTF.

The λ_{CR} values for **2**−**4** were evaluated to be ca. 1 eV (Table 4), which is slightly large compared with that of **1** (0.8 eV) in PhCN.

From the comparison of the λ_{CR} values (0.8−1 eV) with the $-\Delta G_{CR}$ value (ca. 1.3−1.6 eV), the charge recombination processes can be considered to belong in the Marcus "inverted region" in PhCN. These findings support that the radical ion-pairs have long lifetimes. The short τ_{RIP} for **1** cannot be interpreted by the larger energy difference between the λ_{CR} value (0.8 eV) and the ΔG_{CR} value (ca. 1.3 eV) compared with those for **2**−**4** (the λ_{CR} values (0.9−1.0 eV) and the ΔG_{CR} values (ca. 1.3 eV)) in PhCN.

The $|V|_{CR}$ values for **2**−**4** were calculated to be ca. 0.1 cm^{-1} from the first term of eq 3 (intercept of the line at $1/T = 0$ in Figure 8). These $|V|_{CR}$ values are small compared with the reported $|V|_{CR}$ values (1−100 cm^{-1}) for other electron-transfer systems,[15,16] In the case of **1** with the flexible spacers, the $|V|_{CR}$ value was calculated to be ca. 0.4 cm^{-1}, which is larger than those for **2**−**4** with the cyclohexyl spacers. The larger $|V|_{CR}$ value for **1** supports the fast charge-recombination process. Generally, the smaller $|V|_{CR}$ value for the longer spacer between TTF$^{\bullet+}$ and NIm$^{\bullet-}$ in **1** than those for shorter cyclohexyl spacer in **2**−**4** would be anticipated. Thus, it is suggested that the TTF$^{\bullet+}$ moiety becomes closer to the NIm$^{\bullet-}$ moiety with a conformational change accompanying the attraction force between the oppositely charged species in **1**, resulting in the larger $|V|_{CR}$ value. Therefore, the contribution of the through space electron transfer may be considered for such a charge recombination of **1**. For charge separation, on the other hand, such an acceleration effect was not appreciably observed for **1**, because the lifetime of the singlet excited state of **1** is shorter than the lifetime of the ion pair, in addition to the lack of the attraction force between neutral molecules during the conformational change.

Energy Diagram. From the fluorescence spectrum in Figure 2, the energy of the excited singlet state of the NIm moiety is 3.10 eV. The charge-separated states can be calculated to be ca. 1.3 eV in PhCN, which corresponds to ΔG_{CR} in Table 3. Thus, the ΔG_{CS} values via the singlet excited state of the NIm moiety can be evaluated to be ca. −1.8 eV in PhCN, although the ΔG_{CS} and ΔG_{CR} values depend on the R_{cc} and solvent polarity. Thus, an energy diagram can be schematically illustrated as shown in Figure 9. The 355 nm laser excitation (3.52 eV) pumps up the NIm moiety of TTF-(sp)-NIm-(sp)-TTF to its singlet excited energy, from which the charge separation takes place quite efficiently in PhCN, chloroform, and toluene, indicating that a wide polarity of solvents are

effective to charge separation as confirmed by the time-resolved fluorescence measurements (Table 2).

For **1**, a small part of the singlet states of the NIm moiety may be converted to the triplet state, because of the smaller than unity Φ_{CS} value as shown in Table 2. If the energy level of the triplet state of the NIm moiety is higher than that of the charge-separation state, the charge-separation is possible.[17] However, fluorescence lifetime measurements indicate that the fraction of intersystem crossing from singlet states to the triplet state of the NIm moiety is small. Therefore, the fraction of charge separation via the triplet state of the NIm moiety is small. Indeed, the observed sharp rise and decay of $TTF^{\bullet+}$-(sp)-$NIm^{\bullet-}$-(sp)-TTF for **1** in Figure 5 may exclude the triplet route for charge separation. Higher Φ_{CS} values for **2**−**4** further decrease the possibility of the triplet rout.

Comparison with Other Similar Systems. O'Neil et al. observed a super-exchange electron-transfer mechanism for porphyrin-NIm-porphyrin triads with a short spacer.[18,19] In the present study, because we employed the relatively long spacers, such a super-exchange electron mechanism between apart TTF moieties was not expected. For TTF-(sp)-C_{60} with a flexible long chain spacer, it was reported that charge separation takes place via the singlet excited state of C_{60}, producing $TTF^{\bullet+}$-(sp)-$C_{60}^{\bullet-}$; however, the Φ_{CS} value was smaller than that of **1** with a similarly long flexible bond.[8c] The τ_{RIP} of $TTF^{\bullet+}$-(sp)- $C_{60}^{\bullet-}$ was evaluated to be 49 ns in PhCN,[8c] which is almost the same as that of $TTF^{\bullet+}$-(sp)-$NIm^{\bullet-}$-(sp)-TTF for **1**.

Conclusion

In the intramolecular photoinduced charge-separation process, rapid charge separation with high efficiency was found for $TTF^{\bullet+}$-(sp)-$NIm^{\bullet-}$-(sp)-TTF for **2**−**4** with rigid cyclohexyl spacers, whereas a slightly low efficiency was found for the flexible spacer (triad **1**). On the other hand, slower charge recombination was found for $TTF^{\bullet+}$-(sp)-$NIm^{\bullet-}$-(sp)-TTF for **2**−**4** with rigid cyclohexyl spacers than that with a flexible spacer. The reorganization energies and coupling constants evaluated from the temperature effects for the charge-recombination rate constants afford some keys to interpret the observed phenomena.

Acknowledgment. The present research was financially supported by NSFC (90101025), the Chinese Academy of Sciences and State Key Basic Research Program (G2000077500). DZ thanks the National Science Fund for Distinguished Young Scholars. This work was supported by a Grant-in-Aid (Nos. 14350449 & 15033207) from the Ministry of Education, Culture, Sports, Science and Technology, Japan and the Mitsubushi Fundation.

Supporting Information Available: The syntheses and data for the products were summarized. This material is available free of charge via the Internet at http://pubs.acs.org.

References and Notes

(1) (a) Jordan, K. D.; Paddon-Row, M. N. *Chem. Rev.* **1992**, *92*, 395. (b) Wasielewsky, M. R. *Chem. Rev.* **1992**, *92*, 435. (c) Osuka, A.; Mataga, N.; Okada, T. *Pure Appl. Chem*. **1997**, *69*, 797. (d) Verhoeven, J. W. *Adv. Chem. Phys*. **1999**, *106*, 603.

(2) (a) Williams, R. M.; Zwier, J. M.; Verhoeven, J. W. *J. Am. Chem. Soc*. **1995**, *117* (14), 4093−4099. (b) Eckert, J.-F.; Nicoud, J.-F.; Nierengarten, J.-F.; Liu, S.-G.; Echegoyen, L.; Barigelletti, F.; Armaroli, N.; Ouali, L.; Krsnikov, V.; Hadziioannou, G. *J. Am. Chem. Soc.* **2000**, *122*, 7467, (c) Imahori, H.; Sakata, Y. *Eur. J. Org. Chem.* **1999**, *445*, 5. (d) Guldi, D. M.; Prato, M. *Acc. Chem. Res.* **2000**, *33*, 695. (e) Yamazaki, M.; Araki, Y.; Fujitsuka, M.; Ito, O. *J. Phys. Chem. A* **2001**, *105*, 8615.

(3) (a) Davis, W. B.; Ranter, A.; Wasielewsky, M. R. *Chem. Phys*. **2002**, *281*, 333. (b) Sinks, L. E.; Wasielewsky, M. R. *J. Phys. Chem. A* **2003**, *107*, 611. (c) Lukas, A. S.; Bushard, P. J.; Weiss, E. A.; Wasielewsky, M. R. *J. Am. Chem.* Soc. **2003**, *125*, 3921.

(4) (a) He, Z.; Gosztola, D.; Demg, Y.; Goa, G.; Wasielewsky, M. R; Kispert, L. D. *J. Phys. Chem. B* **2000**, *104*, 6668. (b) Lukas, A. S.; Bushard, P. J.; Wasielewsky, M. R. *J. Am. Chem.* Soc. **2001**, *123*, 2440.

(5) (a) Sariciftci, N. S. *Prog. Quantum Electron*. **1995**, *19*, 131. (b) Jensen, A. W.; Wilson, S. R.; Schuster, D. I. *Bioorg. Med. Chem*. **1996**, *4*, 767. (c) Prato, M. *J. Mater. Chem*. **1997**, *7*, 1097. (d) Gust, G.; Moore, T. A.; Moore, A. L. *Res. Chem. Intermed*. **1997**, *23*, 621. (e) Imahahori, H.; Sakata, Y. *Adv. Mater*. **1997**, *9*, 537. (f) Gust, D.; Moore, T. A.; Moore A. L. *Acc. Chem. Res*. **2001**, *34*, 40. (g) Imahori, H.; Mori, Y.; Matano, Y. *J. Photochem. Photobiol. C: Photochem. Rev.* **2003**, *4*, 51.

(6) (a) Ohkochi, M.; Takahashi, A.; Mataga, N.; Okada, T.; Osuka, A.; Yamada, H.; Maruyama, K. *J. Am. Chem.* Soc. **1993**, *115*, 12137. (b) Greenfield, S. R.; Svec, W. A.; Gosztola, D.; Wasielewisky, M. R. *J. Am. Chem.* Soc. **1996**, *118*, 6767. (c) Imahori, H.; Tamaki, K.; Araki, Y.; Hasobe, T.; Ito, O.; Shimomura, A.; Kundu, S.; Okada, T.; Sakata, Y.; Fukuzumi, S. *J. Phys. Chem. A* **2002**, *106*, 2803.

(7) (a) Alam, M. M.; Watanabe, A.; Ito, O. *J. Photochem. Photobiol. A: Chem.* **1997**, *104*, 59. (b) Alam, M. M.; Watanabe, A.; Ito, O. *Bull. Chem. Soc. Jpn*. **1997**, *70*, 1833. (c) Alam, M. M.; Ito, O.; Sakurai, N.; Moriyama, H. *Fullerene Sci. Technol.* **1998**, *6*, 1007. (d) Alam, M. M.; Ito, O.; Sakurai, N.; Moriyama, H. *Res. Chem. Intermed*. **1999**, *25*, 323.

(8) (a) Martín, N.; Sanchez, L.; Herranz, M. A.; Guldi, D. M. *J. Phys. Chem. A* **2000**, *104*, 4648. (b) Herranz, M. A.; Ollescas, B.; Martin, N.; Luo, C.; Guldi, D. M. *J. Org. Chem* **2000**, *65*, 5728. (c) Segura, J. L.; Martín, N. *Angew. Chem., Int. Ed.* **2001**, *40*, 1372. (d) Allard, E.; Cousseau, J.; Orduna, J.; Garin, J.; Luo, H.; Araki, Y.; Ito, O. *Phys. Chem. Chem. Phys.* **2002**, *4*, 5944. (e) Sadaike, S.; Tokimiya, K.; Aso, T.; Otsubo, T. *Tetrahedron Letts*. **2003**, *44*, 161.

(9) (a) Marcus, R. A. *J. Chem. Phys.* **1956**, *24*, 966. (b) Marcus, R. A. *J. Chem. Phys.* **1957**, *26*, 867. (c) Marcus, R. A. *J. Chem. Phys.* **1957**, *26*, 872. (d) Marcus, R. A. *J. Chem. Phys.* **1965**, *43*, 679.

(10) Stewart, J. J. P. J. *Comput. Chem.* **1989**, *10*, 209; *MOPAC* version 7.

(11) (a) Fujitsuka, M.; Ito, O.; Yamashiro, T.; Aso, Y.; Otsubo, T. *J. Phys. Chem. A* **2001**, *104*, 4876. (b) Fujitsuka, M.; Tsuboya, N.; Hamasaki, R.; Ito, M.; Onodera, S.; Ito, O.; Yamamoto, Y. *J. Phys. Chem. A* **2003**, *107*, 1452.

(12) In the observed ^{1}H NMR spectra, it was also difficult to discriminate which configuration is more stable.

(13) (a) Fujitsuka, M.; Luo, C.; Ito, O. *J. Phys. Chem. B* **1999**, *103*, 445. (b) Luo, C.; Fujitsuka, M.; Huang, C.-H.; Ito, O. *Phys. Chem. Chem. Phys.* **1999**, *1*, 2923.

(14) (a) Huchet, L.; Akoudad, S.; Levillain, E.; Roncali, J.; Emge, A.; Bauerle, P. *J. Phys. Chem. A* **1998**, *102*, 7776. (b) Ashton, P. R.; Balzani, V.; Becher, J.; Credi, A.; Fyfe, M. C. T.; Mattersteig, G.; Menzer, S.; Nielsen, M. B.; Raymo, F. M. J.; Stoddart, F.; Venturi, M.; Williams, D. J. *J. Am. Chem.* Soc. **1999**, *121*, 3951. (c) Andreu, R.; Garin, J.; Orduna, J. *Tetrahedron* **2001**, *57*, 7883. (d) Spanggaard, H.; Prehn, J.; Nielsen, M. B.; Levillain, E.; Allain, M.; Becher, J. *J. Am. Chem.* Soc. **2000**, *122*, 9486.

(15) (a) Luo, C.; Guldi, D. M.; Imahori, H.; Tamaki, K.; Sakata, Y. *J. Am. Chem. Soc*. **2000**, *122*, 6535. (b) Fukuzumi, S.; Imahori, H.; Yamada, H.; El-Khouly, M. E.; Fujitsuka, M.; Ito, O.; Guldi, D. M. *J. Am. Chem. Soc*. **2001**, *123*, 2571. (c) Imahori, H.; Tamaki, K.; Guldi, D. M.; Luo, C.; Fujitsuka, M.; Ito, O.; Fukuzumi, S. *J. Am. Chem. Soc*. **2001**, *123*, 2607. (d) Imahori, H.; Guldi, D. M.; Tamaki, K.; Yoshida, Y.; Luo, C.; Sakata, Y.; Fukuzumi, S. *J. Am. Chem. Soc*. **2001**, *123*, 6617. (e) Imahori, H.; Tamaki, K.; Araki, Y.; Sekiguchi, Y.; Ito, O.; Sakata, Y.; Fukuzumi, S. *J. Am. Chem. Soc.* **2002**, *124*, 5165.

(16) (a) Lindell, P. A.; Kuciauskas, D.; Sumida, J. P.; Nash, B.; Nguyen, D.; Moore, A. L.; Moore, T. A.; Gust, D. *J. Am. Chem. Soc*. **1997**, *119*, 1400. (b) Carbonera, D.; Di Valentin, M.; Corvaja, C.; Agostini, G.; Giacometti, G.; Liddell, P. A.; Kuciauskas, D.; Moore, A. L.; Moore, T. A.; Gust, D. *J. Am. Chem. Soc.* **1998**, *120*, 4398.

(17) Rogers, J. E.; Kelly, L. A. *J. Am. Chem. Soc*. **1999**, *121*, 3854.

(18) O'Neil, M. P.; Niemczky, M. P.; Svec, W. A.; Gosztola, D.; Gaines, G. L., III.; Wasielewsky, M. R. *Science* **1992**, *257*, 63.

(19) Redmore, N. P.; Rubtsov, I. V.; Therien, M. J. *J. Am. Chem.* Soc. **2003**, *125*, 8769.